7.10 EVALUATING NEW CLOUD-RADIATION AND HYDROLOGIC CYCLE PARAMETERIZATIONS

Sam F. Iacobellis* and Richard C. J. Somerville

Scripps Institution of Oceanography, University of California, San Diego

1. INTRODUCTION

Precipitation within clouds is initiated by a variety of processes, including the collision and coalescence of cloud droplets in liquid water clouds and the Bergeron-Findeisen process in mixed-phase clouds. This is generally referred to as the auto-conversion process and must be parameterized in atmospheric general circulation models (GCMs).

Most modern GCMs now include prognostic cloud parameterizations that treat cloud fraction and cloud water/ice amount as interactive variables. These cloud water/ice amounts are used to prognostically calculate the cloud optical properties that can have a large influence on the model's radiation budget. Thus, the accurate parameterization of the auto-conversion process is important for both modeling of precipitation rates and specification of cloud optical properties (Liu and Daum, 2004; Rotstayn 2000).

There are several auto-conversion parameterizations currently being used in GCMs. Many of these are based on the parameterization originally devised by Kessler (1969) in which the precipitation rate is linearly proportional to the cloud water content once the cloud water content exceeds a specified threshold value. There have been many derivations of this scheme (see Liu and Daum, 2004) including ones by Manton and Cotton (1977) and Liou and Ou (1989). Other schemes such as that of Sundqvist et al (1989) parameterize the precipitation rate as a continuous exponential function of the cloud water content.

In a recent paper, Xu et al (2004) found that single-column models (SCMs) using a Sundqvist type auto-conversion parameterization drastically underestimated the cloud liquid water content during a 27-hour study period within the March 2000 Atmospheric Radiation Measurement (ARM) Program's Intensive Operation Period (IOP) at the Southern Great Plains (SGP) site. Their results also suggest that models using the Manton-Cotton auto-conversion scheme performed much better during this time period.

In this paper we analyze results from separate runs of a SCM using these two auto-conversion parameterizations. The SCM and the auto-conversion parameterizations are discussed in future detail in section 2. The data used to evaluate the model results are described in section 3. In section 4, the results are first analyzed over the 27-hour period used by Xu et al (2004) and are then compared over longer time periods and during specific meteorological conditions. The sensitivity of the model results to the specification of the cloud droplet number concentration is also examined. The goal of this analysis is to determine if indeed one type of auto-conversion produces more realistic results for a variety of times and meteorological conditions at the SGP site. Section 5 contains a discussion of the model results and examines the implications of these results.

* Corresponding author address: Sam F. Iacobellis, Scripps Institution of Oceanography, La Jolla, CA 92093-0224; e-mail: siacobellis@ucsd.edu.

2. MODEL

The SCM is an isolated column of atmosphere extending upwards from, and including, the underlying surface. The SCM utilizes 53 layers and thus has a relatively high vertical resolution in comparison to most GCMs. The horizontal extent of the SCM domain is approximately 200 x 250 km and represents the Cloud and Radiation Testbed (CART) at the ARM SGP site. This SCM was used by Iacobellis et al (2003) and is related closely to the "Scripps SCM" that participated in the SCM comparison studies of Ghan et al (2000) and Xie et al (2002).

The control version of the SCM contains the Rapid Radiation Transfer Model (RRTM) longwave radiation transfer scheme described by Mlawer et al (1997) and the CCM3 shortwave radiation parameterization (Briegleb, 1992). The convection scheme is the CCM3 mass flux parameterization (Zhang and McFarlane, 1995; and Hack, 1994).

Cloud amount and cloud water/ice are prognostic variables and are parameterized using the scheme of Tiedtke (1993). Terms representing the formation of clouds and cloud water/ice due to convection, boundary layer turbulence and stratiform condensation processes are included in this parameterization. Cloud water/ice is removed through evaporation and conversion of cloud droplets and ice to precipitation (details described below). Ice particle settling is included in the SCM with individual crystal fall speeds calculated from Mitchell (1996) as described in Ivanova et al (2001). Typical fall speeds range from 0.25 to 1.0 m sec^{-1}. Maximum cloud overlap has been assumed throughout this study.

The shortwave optical properties of clouds are parameterized using the schemes of Slingo (1989) for liquid water clouds and McFarquhar et al (2002) for ice clouds. Ice particle effective radius (R_{eff}) is determined using the parameterization described in McFarquhar (2001), while the effective radius of liquid droplets is calculated following Bower et al (1994).

2.1 *Auto-conversion Schemes*

The focus of this paper is on the auto-conversion process that takes place inside of liquid water clouds. As a result, no changes are made to the auto-conversion parameterization for ice clouds. The Tiedtke (1993) cloud parameterization used in the SCM employs a Sundqvist et al (1989) type scheme for ice clouds (see below) that includes parameters that take into account the Bergeron-Findiesen process and ice crystal growth within cirrus clouds. In the mixed-phase region, the total auto-conversion of cloud water to precipitation is simply a linear combination of the liquid and ice components using the fraction of ice (f_{ice}):

$$G_{p,tot} = (1 - f_{ice})G_{p,liq} + f_{ice}G_{p,ice} \quad (1)$$

where fice is the fraction of cloud water that is ice,

$$\begin{aligned} f_{ice} &= 0.0 && T \geq 0C \\ f_{ice} &= -T/16 && 0C > T > -16C \\ f_{ice} &= 1.0 && T \leq -16C \end{aligned} \quad (2)$$

2.1.1 *Sundqvist*

The conversion of cloud water to precipitation developed by Sundqvist et al (1989) and later used by Tiedtke (1993) is parameterized as

$$G_{p,liq} = \frac{\rho_a l_c}{c_0}\left[1 - \exp\left(-\left(\frac{l_c}{l_{crit}}\right)^2\right)\right], \quad (3)$$

where c_0^{-1} is a characteristic time scale for conversion of cloud droplets into raindrops, r_a is the density of air, l_c is the cloud water content averaged per cloud area (in-cloud value), and l_{crit} represents a typical cloud water content at which the release of precipitation begins to be efficient. The parameters c_0 and l_{crit} are adjusted to take into account coalescence due to precipitation falling through the cloud and the Bergeron-Findeisen process. Tiedtke (1993) uses values (stratiform case) of c_0=10^{-4} sec^{-1} and l_{crit}=3x10^{-4} kg kg^{-1}.

2.1.2 *Manton-Cotton*

Manton and Cotton (1977) proposed a parameterization for the conversion of cloud water to precipitation that is based on the original Kessler (1969) scheme, but includes the effect of the cloud droplet concentration:

$$G_{p,liq} = f_c l_c H(l_c - l_{cm}), \quad (4)$$

where f_c represents a mean collision frequency of cloud droplets that become rain drops, H is the Heaviside step function, and l_{cm} is a threshold cloud water content below which there is negligible conversion of cloud water to rain. Manton and Cotton (1977) express f_c as

$$f_c = \pi r_c^2 E_c V_c N_c, \quad (5)$$

where r_c is the mean volume radius, E_c is the average collection efficiency, V_c is the terminal velocity of a droplet with radius r_c, and N_c is the mean cloud water droplet concentration. The mean volume radius defined as

$$r_c^3 = 0.75\pi(l_c/\rho_w)N_c, \quad (6)$$

where ρ_w is the density of water. The threshold cloud water content is a function of the mean volume radius such that

$$l_{cm} = (4\pi/3)\rho_w r_{cm}^3 N_c \quad (7)$$

with r_{cm} being the threshold mean droplet radius. Manton and Cotton used values E_c=0.55 and r_{cm}=10 μm. Unless otherwise specified, the value of N_c is set to 200 cm^{-3} which is a typical value for continental conditions. The sensitivity of model results to the N_c is examined in Section 4.3. Note that as written in the above equations, $G_{p,liq}$ is an in-cloud value and needs to be multiplied by the cloud fraction to obtain a grid-mean value.

2.2 *Forcing Data*

In this study, the SCM is forced with time-dependent horizontal advective fluxes of heat, moisture and momentum from the European Centre for Medium-Range Weather Forecasting (ECMWF) that are supplied specially for the ARM Program sites (ECMWF, 2002). The surface temperature and surface heat fluxes were also specified from the ECMWF data.

A series of SCM runs were performed, with the starting time of each run spaced 6 hours apart. Each individual SCM run is 36 hours in length, the first 12 hours being a spin-up period where the model temperature and humidity are specified from the ECMWF analysis. The spin-up period is used to allow the SCM cloud variables to reach a *quasi* steady state. After the spin-up period, the SCM temperature and humidity are no longer constrained. Only the last 24 hours of each SCM run is used in the analysis.

The SCM results from all runs are averaged together, thus the model values at any given time are a mean from 4 runs. The staggering of SCM start times by 6 hours (rather than say 24 hours) is to insure that the time of day at start up does not influence the results. Additionally, this method also insures that the results at a given time of day are not always at the end (or beginning) of the model run.

3. OBSERVATIONAL DATA

3.1 *Liquid Water Path*

Measurements of liquid water path (LWP) were obtained from data collected by five Microwave Radiometers (MWR) located within the ARM SGP site. The MWR instrument measures the microwave emissions of liquid water molecules at a frequency of

31.4GHz from which the LWP is calculated. The presence of precipitation causes unrealistic values in the retrieved LWP (Sheppard, 1996), thus time periods in which precipitation occurred are ignored. Since the LWP values would tend to be highest during precipitation periods, the long-term averages from the MWR instrument calculated here may underestimate the actual value of LWP.

3.2 *LWC and Cloud Frequency Profiles*

Liquid water content data at the SGP site is derived from Millimeter Cloud Radar (MMCR) and MWR data together with a relationship relating radar reflectivity to water content. The MMCR data is obtained from the Active Remotely-Sensed Cloud Locations (ARSCL) product available from the ARM data archive (www.arm.gov/data/). The MMCR operates at the SGP Central Facility and produces data with a temporal resolution of 10 seconds and vertical resolution of 45 meters.

For each time record, the radar reflectivity is used to compute cloud water content via the formula of Sassen and Liao (1994) for liquid and Liu and Illingworth (2000) for ice:

$$LWC = \left(\frac{N_c}{3.6} Z\right)^{1.0/1.8} \quad (8)$$

$$IWC = 0.097 Z^{0.59} \quad (9)$$

where Z is the radar reflectivity in mm^6/m^3, N_c is the cloud droplet concentration (cm^{-3}), and LWC and IWC are in g m^{-3}. Sassen and Liao (1994) found best agreement with empirical research using a value of N_c=100 cm^{-3}. We note that this value differs from the value of N_c used in the SCM.

At each radar height level, the observed temperature and Eq. (2) are used to determine the whether the cloud is liquid, ice or a mixture of both. Note that this is different from the alternative approach that uses the temperature to separate the *reflectivity* into a liquid and ice component. Here, we use the temperature to separate the *total cloud water* into liquid and ice components. The present approach entails an additional iterative procedure to determine total cloud water that when divided into the liquid and ice fractions produces a total reflectivity using (8) and (9) that matches the reflectivity measured by the MMCR.

For each radar retrieval, the liquid water path (LWP_{rad}) is computed using the values of LWC obtained from (8). The LWC values are then scaled using the scaling factor, $f = LWP_{mwr}/LWP_{rad}$, where LWP_{mwr} is the liquid water path obtained the MWR instrument that is co-located with the MMCR instrument. Thus the shape of the LWC profile is determined by the radar measurements, while MWR measurements specify the magnitude of the values.

The ARSCL product also contains a vertical profile of cloud occurrence for each radar retrieval. In the cloud profile results presented in section 4, the base height of the lowest cloud layer was estimated using multipulse lidar measurements which minimizes the effect of larger hydrometeors and helps eliminate false cloud signals due to falling precipitation.

4. RESULTS

The SCM was run with both the Sundqvist auto-conversion (SCM-S) and Manton-Cotton (SCM-MC) auto-conversion schemes and the results are discussed below for a variety of different time periods. In the discussion that follows, SCM results representing a grid box mean are compared to data from the MMCR that represents a point measurement. Both the SCM and MMCR data are time-averaged over a period of at least 24 hours. This helps to some extent in making a comparison between point measurements and grid-mean values, however it should still be kept in mind that there may be discrepancies between the two types of data.

4.1 *27-hour Period During March 2000 SGP IOP*

The evolution of the column liquid water path from model runs SCM-S and SCM-MC are shown in Figure 1 together with the observed value computed by averaging measurements from the 5 individual MWR locations within the SGP site. Throughout the 27-hour period (0300Z March 17 to 0600Z March 18) run SCM-MC produces significantly larger values of LWP than run SCM-S. The LWP results from SCM-MC are also much closer to the measured values from the MWR data during much of the 27-hour period.

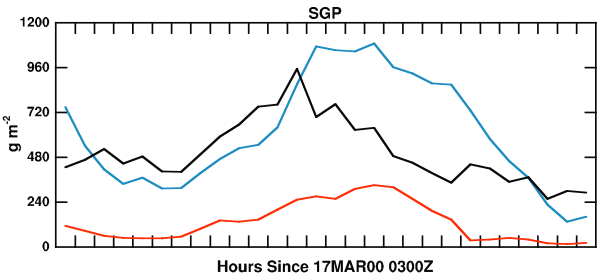

Figure 1. Time evolution of *LWP* from SCM-S (red), SCM-MC (blue) and MWR measurements (black) during the 27-hour period 0300Z March 17 to 0600Z March 18.

The vertical profiles of cloud fraction and cloud liquid water content (grid-mean and in-cloud values) are shown in Figure 2 from both SCM runs and from MMCR derived measurements. The magnitude of LWC from SCM-MC is much closer to the MMCR data than the results from SCM-S, however the shape of the LWC profile from either run does not compare well with the MMCR measurements. This is true for both the grid-mean and in-cloud values. Additionally, the maximum cloud fraction from both SCM runs is about 1 km higher than the MMCR data indicates. While vertically displaced, the maximum cloud fraction from SCM-MC is closer to the measured cloud fraction maximum compared to the results from SCM-S.

The two SCM runs produce strikingly different precipitation amounts during this 27-hour period. These amounts along with ARM precipitation measurements are shown in Figure 3. Run SCM-S produces significantly more precipitation than SCM-MC during this period. Additionally, SCM-S produces a smoother evolution of precipitation than does SCM-MC. These differences are due to the nature of the two auto-conversion schemes. The Sundqvist auto-conversion scheme is quicker to convert cloud water to precipitation than the Manton-Cotton scheme, resulting in smaller cloud water values and larger precipitation amounts in SCM-S compared to SCM-MC. Also, the use of a threshold liquid cloud water amount (l_{cm}) in the Manton-Cotton scheme results in more "spikiness" in the precipitation.

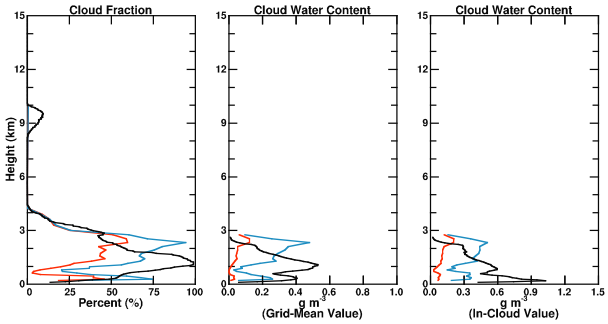

Figure 2. Mean vertical profiles of cloud fraction, grid-mean *LWC* and in-cloud *LWC* from run SCM-S (red), SCM-MC(blue), and MMCR derived measurements (black) during the 27-hour period 0300Z March 17 to 0600Z March 18.

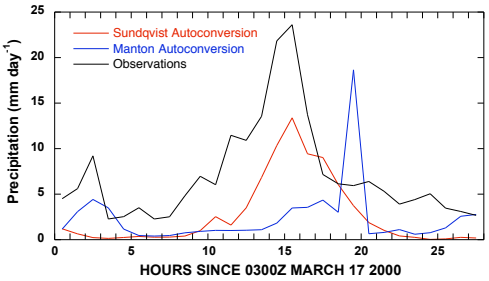

Figure 3. Time series of the precipitation rate from SCM-S (red), SCM-MC (blue), and ARM surface measurements (black) during the 27-hour period 0300Z March 17 to 0600Z March 18.

4.2 *Monthly and Seasonal Timescales*

The 27-hour period examined above was selected in Xu et al (2004) due to the shallow frontal cloud systems observed at the SGP during this time. However, the results from the SCM runs during this period may not be representative of other time periods. In this section, SCM results are examined on monthly and seasonal timescales.

The evolution of the daily mean column liquid water paths from SCM-S and SCM-MC were examined along with MWR measurements for each month in the year 2000 (daily means from March 2000 are shown in Figure 4). It is evident from this data that the results from the 27-hour period discussed in the above section are not representative of other time periods. The LWP results from model run SCM-S are in much closer agreement with the MWR measurements than the results from SCM-MC which tend to significantly overestimate the LWP. This overestimation of the LWP in SCM-MC is clearly seen when the monthly means are plotted (Figure 5).

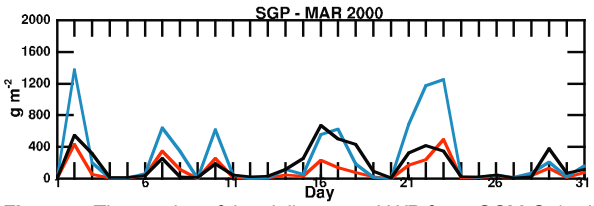

Figure 4. Time series of the daily mean *LWP* from SCM-S (red), SCM-MC (blue), and MWR measurements (black) during March 2000.

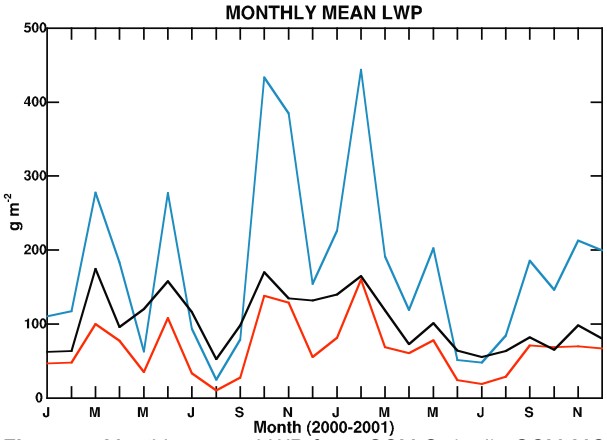

Figure 5. Monthly mean *LWP* from SCM-S (red), SCM-MC (blue), and MWR measurements (black) during 2000-2001.

The mean vertical profiles of cloud fraction and liquid water content averaged on seasonal timescales from both the SCM runs and MMCR measurements are shown in Figure 6. The SCM runs reproduce the general shape and magnitude of the measured cloud fraction profile in all seasons. However, in three of the four seasons the cloud radar measurements indicate a relative cloud maximum in the lowest 2 km. that the SCM results either underestimate or miss altogether.

The differences in cloud water content between the two SCM runs are more pronounced than the cloud fraction differences. Model run SCM-MC consistently overestimates the liquid water content compared to the MMCR measurements. Model run SCM-S produces a mean cloud water content that is closer in magnitude to the MMCR measurements. However, the shape of the SCM-S profile generally underestimates the LWC in the lowest 2-3 km and overestimates the LWC above the 3 km level. Part of this is probably related to the SCM not reproducing the low cloud maximum seen in the MMCR cloud fraction data. Another possible cause are errors in the MMCR retrieval due to the presence of both liquid and ice water in the region above 3 km. A linear relationship based on temperature was used in the retrieval algorithm (same as in the SCM) to separate liquid

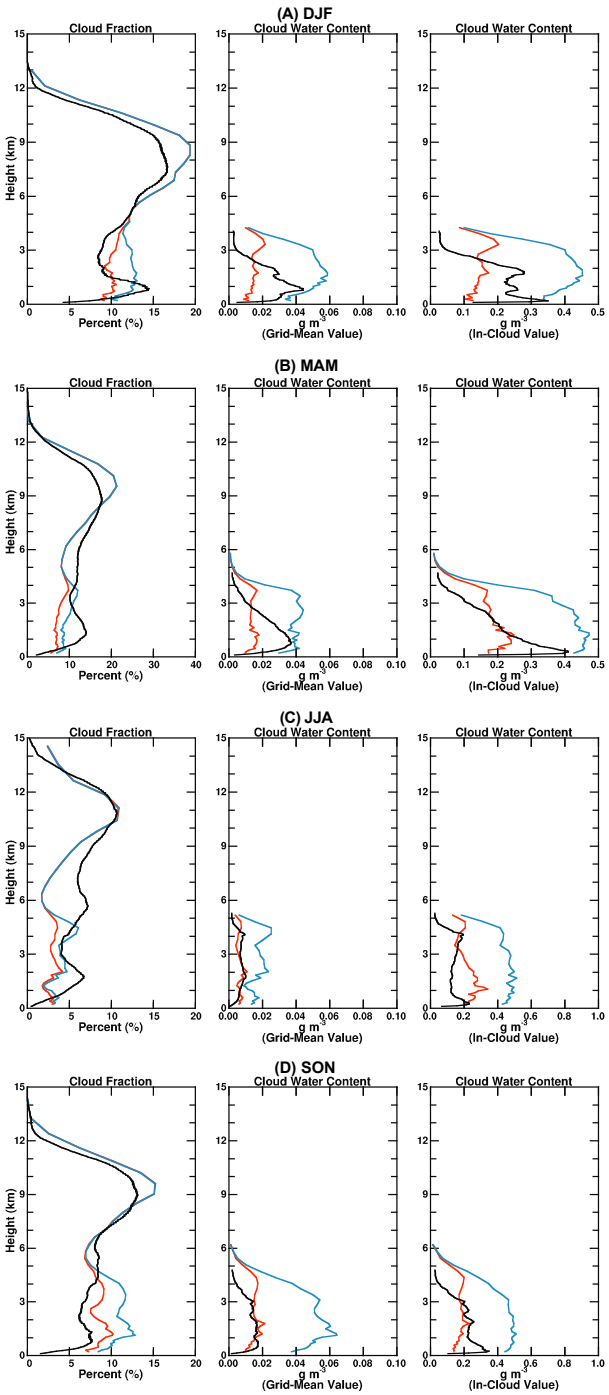

Figure 6. Seasonal mean vertical profiles of cloud fraction, grid-mean *LWC*, and in-cloud *LWC* from SCM-S (red), SCM-MC (blue), and MMCR derived measurements (black) during (a) winter, (b) spring, (c) summer, and (d) autumn.

water from ice. Since the radar reflectivity is vastly different for ice particles and liquid water droplets, an error in the partitioning of the mixed phases could lead to significant errors in the retrieved amounts of liquid and ice water contents. Despite these possible errors, it is clear that the mean LWC from run SCM-MC significantly overestimates the measured values.

The 27-hour time-span examined in section 4.1 was a period of shallow frontal clouds at the SGP site. To isolate those times when shallow cloud layers are present at the SGP, we now only include those times when there are shallow clouds present in both the SCM and measured cloud data. Here, shallow is defined as between the surface and 3 km, with no overlying clouds of thickness greater than 1000 m. These means are shown in Figure 7 for the months of November to March as these conditions rarely occurred simultaneously in the SCM and observational data during the months April to October. The results from SCM-MC compare much better to the measured values of LWC when only these instances of shallow clouds are retained. As in Fig. 6, the shape of the SCM profiles does not agree with the measured profiles, but the overall magnitude is much better simulated by run SCM-MC.

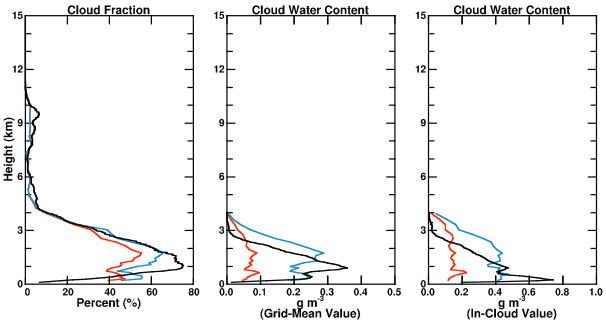

Figure 7. Seasonal mean vertical profiles of cloud fraction, grid-mean *LWC*, and in-cloud *LWC* from SCM-S (red), SCM-MC (blue), and MMCR derived measurements (black) during the months of November - March. Only those times when shallow clouds are present with no overlying clouds are included in the averages

Figure 8 contains the mean profiles of cloud fraction and liquid water content for those periods in which there were both shallow clouds and higher clouds present in both the SCM and measured cloud data. Here the liquid water content profiles from SCM-S are much closer to the observed values than the profiles from SCM-MC. This suggests that the presence of high clouds above the shallow clouds may have some influence on the modeled and/or observed cloud water content profiles. This possibility is discussed further in section 5.

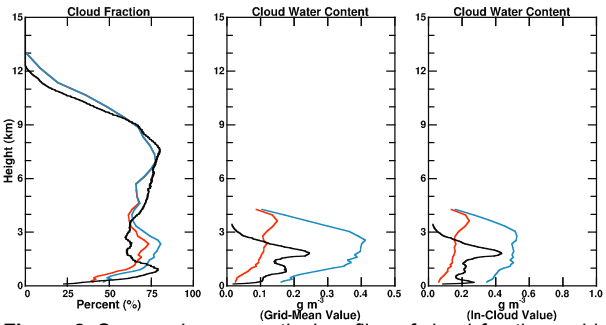

Figure 8. Seasonal mean vertical profiles of cloud fraction, grid-mean *LWC*, and in-cloud *LWC* from SCM-S (red), SCM-MC (blue), and MMCR derived measurements (black) during the months of November - March. Only those times when shallow clouds and higher clouds are present are included in the averages.

4.3 *Sensitivity to N_c*

Miles et al. (2000) constructed a database of liquid water cloud droplet size parameters derived from *in situ* data reported in existing literature. For continental stratocumulus, they found a wide range of N_c, with the vast majority of observations between 50 and 600 cm^{-3}.

SCM-MC was rerun several times during March 2000, each time using a different constant value of the cloud droplet concentration N_c ranging from 100 to 600 cm^{-3}. The mean vertical profiles of cloud fraction and liquid water content from these runs are shown in Figure 9. These results illustrate that the SCM results are very sensitive to the specification of N_c (for comparison, the value of N_c used in the earlier runs of SCM-MC was set to 200 cm^{-3}). The mean value of the liquid water content approximately doubles for a doubling of N_c. The mean cloud fraction also increases with N_c. This has an important impact on the radiative fluxes as not only are there more clouds with higher values of N_c, but the cloud optical thicknesses are also larger (larger values of N_c and *LWC* would both increase the optical thickness).

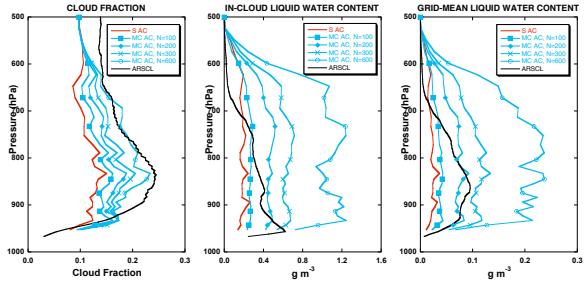

Figure 9. Mean vertical profiles of cloud fraction, in-cloud *LWC*, and grid-mean *LWC* during March 2000. Results from SCM-S are shown in red, while results from several runs of SCM-MC with varying values of N_c are shown in blue. Values derived from MMCR measurements are shown in black.

Table 1 shows the differences in the top of atmosphere (TOA) cloud forcing terms from these runs along with satellite observations. The value of the shortwave cloud forcing term varies by 10 W m^{-2} for the range of N_c examined here, and 5 W m^{-2} for a more realistic range of N_c = 100 to 300 cm^{-3} (see discussion in section 5). The discrepancy between the modeled and observed cloud forcing is in part due to the SCM generally overestimating the amount of high clouds and underestimating the amount of low clouds during March 2000.

	LW Cloud Forcing (W m^{-2})	SW Cloud Forcing (W m^{-2})
SCM-S	29.5	-54.3
SCM-MC (N_c =100 cm^{-3})	29.9	-57.8
SCM-MC (N_c =200 cm^{-3})	30.7	-60.5
SCM-MC (N_c =300 cm^{-3})	31.3	-62.6
SCM-MC (N_c =600 cm^{-3})	32.2	-67.5
OBS (GOES-XX)	23.1	-66.9

Table 1. The longwave and shortwave TOA cloud forcing values for March 2000 from SCM runs and GOES satellite observations.

5. DISCUSSION

The systematically higher values of *LWC* and cloud fraction produced by SCM-MC (N_c = 200 cm^{-3}) relative to run SCM-S have an impact on the TOA total cloud forcing of about 5 W m^{-2} for March 2000 and 4 W m^{-2} for the entire 2000-2001 period. The primary sensitivity is in the shortwave term as the liquid water clouds in the lower troposphere do not have a strong influence on the TOA longwave cloud forcing.

There were periods when SCM-MC produced more realistic results of cloud LWC (relative to the MMCR derived values) while at other times the results from SCM-S were more realistic. One possible explanation for this inconsistency is that the cloud droplet concentration varies enough in time to cause the differences in the realism of the SCM-MC results.

During the March 2000 IOP at the ARM SGP site, measurements of N_c in liquid water clouds (primarily stratus) were collected by the University of North Dakota Citation research aircraft using a Forward Scattering Spectrometer Probe (FSSP) instrument. The FSSP was configured to count individual cloud particles in 15 size-bins with bin midpoints ranging from about 4 to 60 □m. Correction algorithms were applied to the raw FSSP data to account for probe activity and coincidence (Baumgardner et al. 1985).

Individual flights into liquid water clouds were made on March 3, 17, 18, 19, and 21 with daily mean values of N_c ranging from about 100 to 320 cm^{-3}. For each of these days, SCM-MC was rerun using the measured daily mean N_c. However, the results of these experiments (not shown) show no improvement in the modeled cloud *LWC* compared to the model run using a constant value of N_c =200 cm^{-3}.

Another possible explanation is that overhead clouds could be precipitating into the lower cloud layer increasing the precipitation efficiency of the lower clouds. When these higher clouds are not present, the cloud water in the lower clouds is able to reach a higher value before the onset of precipitation. (Note: the Tiedtke cloud scheme used in SCM includes a term for coalescence due to precipitation falling into a cloudy layer, but it does not attempt to parameterize the Bergeron-Findeisen process that would occur if frozen precipitation falls through a layer containing liquid water cloud droplets). If true, this suggests that this process is underestimated in the SCM and that the Sundqvist auto-conversion compensates for this underestimation to some extent. Additional research is necessary to determine if this is a plausible explanation.

6. CONCLUSIONS

• During the 27-hour period examined by Xu et al (2004), SCM results using the Manton-Cotton auto-conversion parameterizations are more realistic than those results from SCM runs using a Sundqvist type auto-conversion.

• However, over longer time periods the SCM performs better when the Sundqvist auto-conversion scheme is used.

• Analysis indicates that the Manton-Cotton parameterization is more realistic during those periods characterized by shallow low clouds without overlying high clouds.

• SCM results using the Manton-Cotton scheme are particularly sensitive to the specification of the cloud droplet concentration, N_c.

• Future work will explore whether the presence of high clouds has a significant effect on the precipitation efficiency within underlying lower clouds.

7. ACKNOWLEDGMENTS

This research was supported in part by the Office of Science (BER), U. S. Department of Energy under Grant DOEDE-FG02-97-ER62338 and the National Oceanic and Atmospheric Administration under Grant NA77RJ0453.

8. REFERENCES

Baumgardner, D., W. Strapp, and J. E. Dye, 1985: Evaluation of the forward scattering spectrometer probe. Part II: Corrections for coincidence and dead-time losses. *J. Atmos. Oceanic Technol.,* **2**, 626-632.

Bower, K. N., T. W. Choularton, J. Latham, J. Nelson, M. B. Baker, and J. Jenson, 1994: A parameterization of warm clouds for use in atmospheric general circulation models. *J. Atmos. Sci.*, **51**, 2722-2732.

Briegleb, B. P., 1992: Delta-Eddington approximation for solar radiation in the NCAR Community Climate Model. *J. Geophys. Res.*, **97**, 7603-7612.

ECMWF, 2002: The ECMWF operational analysis and forecasting system: The full evolution http://www.ecmwf.int/products/data/operational_system/index.html

Ghan, S., and co-authors, 2000: A comparison of single column model simulations of summertime midlatitude continental convection. *J. Geophys. Res.*, **105**, 2091-2124.

Hack, J. J., 1994: Parameterization of moist convection in the National Center for Atmospheric Research community climate model (CCM2). *J. Geophys. Res.*, **99**, 5551-5568

Iacobellis, S. F., G. M. McFarquhar, D. L. Mitchell, and R. C. J. Somerville, 2003: The sensitivity of radiative fluxes to parameterized cloud microphysics. *J. Climate*, **16**, 2979-2996.

Ivanova, D. C., D. L. Mitchell, W. P. Arnott, and M. Poellot, 2001: A GCM parameterization for bimodal size spectra and ice mass removal rates in mid-latitude cirrus clouds. *Atmos. Res.*, **59**, 89-113.

Kessler, E., 1969: *On the Distribution and Continuity of Water Substance in Atmospheric Circulation. Meteor. Monogr.,* **32**, *Amer. Meteor. Soc.,*84 pp.

Liou, K. N., and S. C. Ou, 1989: The role of cloud microphysical processes in climate: An assessment from a one-dimensional perspective. *J. Geophys. Res.*, **94D**, 8599-8607.

Liu, Y., and P. H. Daum, 2004: Parameterization of the autoconversion process. Part I: Analytical formulation of the Kessler-type parameterizations. *J. Atmos. Sci.,* **61,** 1539-1548.

Liu, C.-L., and A. J. Illingworth, 2000: Toward more accurate retrievals of ice water content from radar measurements of clouds. *J. Appl. Meteor.*, **39**, 1130-1146.

Manton, M. J., and W. R. Cotton, 1977: Formulation of approximate equations for modeling moist deep convection on the mesoscale. *Atmos. Sci. Paper, No. 266*, Dept. Atmos. Sci., Colorado State University, Fort Collins, CO.

McFarquhar, G. M., 2001: Comments on 'Parameterization of effective sizes of cirrus-cloud particles and its verification against observation' by Zhian Sun and Lawrie Rikus (October B, 1999, 125, 3037-3055). *Q. J. R. Meteor. Soc.*, **127**, 261-265.

McFarquhar, G. M., P. Yang, A. Macke, and A. J. Baran, 2002: A new parameterization of single-scattering solar radiative properties for tropical ice clouds using observed ice crystal size and shape distributions. *J. Atmos. Sci.*, **59**, 2458-2478.

Miles, L. N., J. Verlinde, and E. E. Clothiaux, 2000: Cloud droplet size distributions in low-level stratiform clouds. *J. Atmos. Sci.*, **57**, 295-311.

Mitchell, D. L., 1996: Use of mass- and area-dimensional power laws for determining precipitation particle terminal velocities. *J. Atmos. Sci.*, **53**, 1710-1723.

Mlawer, E. J., S. J. Taubman, P. D. Brown, M. J. Iacono, and S. A. Clough, 1997: Radiative transfer for inhomogeneous atmospheres: RRTM, a validated correlated-k model for the longwave. *J. Geophys. Res.*, **102**, 16663-16682.

Rotstayn, L. D., B. F. Ryan, and J. J. Katzfey, 2000: A scheme for calculation of the liquid fraction in mixed-phase stratiform clouds in large-scale models. *Mon. Wea. Rev.*, **128**, 1070-1088.

Sassen, K., and L. Liao, 1996: Estimation of cloud content by W-band radar. *J. Appl. Meteor.,* **35**, 932-938.

Slingo, A., 1989: A GCM parameterization for the shortwave radiative properties of water clouds. *J. Atmos. Sci.*, **46**, 1419-1427.

Sheppard, B. E., 1996: Effect of rain on ground-based microwave radiometric measurements in the 20-90 GHz range. *J. Atmos. Oceanic Technol.,* **13**, 1139-1151.

Sundqvist, H., E. Berge, and J. E. Kristjansson, 1989: Condensation and cloud parameterization studies with a mesoscale numerical weather prediction model. *Mon. Wea. Rev.*, **117**, 1641-1657.

Tiedtke, M., 1993: Representation of clouds in large-scale models. *Mon. Wea. Rev.*, **121**, 3040-3061.

Xie, S., and co-authors, 2002: Intercomparison and evaluation of cumulus parameterizations under summertime midlatitude continental conditions. *Q. J. R. Meteorol. Soc.*, **128**, 1095-1135.

Xu, K.-M., and co-authors, 2004: Modeling springtime shallow frontal clouds with cloud-resolving and single-column models. Accepted for publication in the *J. Geophys. Res. - Atmos.*

Zhang, G. J., and N. A. McFarlane, 1995: Sensitivity of climate simulations to the parameterization of cumulus convection in the Canadian Climate Centre general circulation model. *Atmos.-Ocean,* **33**, 407-446.